

28. Duplessy, J. C., Delibrias, G., Turon, J. L., Pujol, C. and Duprat, J., De glacial warming of the northeastern Atlantic Ocean: correlation with the palaeoclimatic evolution of the European continent. *Paleogeogr. Paleoclimatol. Palaeoecol.*, 1981, **35**, 121–144.
29. Sharma, M. and Owen, L. A., Quaternary glacial history of the Garhwal Himalayas, India. *Quat. Sci. Rev.*, 1996, **15**, 335–365.
30. Phadtare, N. R., Sharp decrease in summer monsoon strength 4000–3500 cal yr BP in the central higher Himalays of India based on pollen evidences from alpine peat. *Quat. Res.*, 2000, **53**, 122–129.
31. Chauhan, O. S., Past 20,000-year history of Himalayan aridity: Evidenced from oxygen isotope records in the Bay of Bengal. *Curr. Sci.*, 2003, **84**, 90–93.
32. Sharma, C., Chauhan, M. S., Gupta, A. and Rajagopalan, G., Vegetation and climate of Garhwal Himalayas during last 4000 years BP. In Symposium on Recent Advances in Geological Studies of Northwest Himalaya and Foredeep, Geological Survey of India, Lucknow, 1995, abstr. vol., p. 90.
33. Rostek, F., Bard, E., Beafort, L., Sonzogni, C. and Ganssen, G., Sea surface temperature and productivity records for the past 240 kyr in the Arabian Sea. *Deep-Sea Res. II*, 1997, **44**, 1461–1480.
34. Sonzogni, C., Bard, E. and Rostek, F., Tropical sea-surface temperatures during the last glacial period: a view based on alkenones in Indian Ocean sediments. *Quat. Sci. Rev.*, 1998, **17**, 1185–1201.
35. Kudraas, H. R., Hofman, A., Dooze, H., Emeis, K. and Erlenkueser, H., Modulation and amplification of climate changes in Northern Hemisphere by Indian summer monsoon during the past 80 ky. *Geology*, 2001, **29**, 63–66.
36. Shetye, S. R., Shenoi, S. S. C., Gouveia, A. D., Michael, G. S., Sundar, D. and Nampoothri, G., Wind driven coastal upwelling along the western boundary of the bay of Bengal during southwest monsoon. *Continental Shelf Res.*, 1991, **11**, 1397–1408.
37. Shetye, S. R., Gouveia, A. D., Shenoi, S. S. C., Sundar, D., Michael, G. S. and Nampoothri, G., The western boundary current in the seasonal subtropical gyre in the Bay of Bengal. *J. Geophys. Res.*, 1993, **98**, 945–954.
38. Sharma, S. *et al.*, Late glacial and Holocene environmental changes in Ganga plain, Northern India. *Quat. Sci. Rev.*, 2004, **23**, 145–159.
39. Weaver, C. E., *Clays, Muds and Shales*, Elsevier, Amsterdam, 1989, p. 819.
40. Konta, J., In *Mineralogy and Chemical Maturity of Suspended Matter in Major Rivers Samples under SCOPE/UNEP, Transport of Carbon and Minerals in Major World Rivers. Part III* (eds Degens, T. and Kempe, S.), Mitteilungen aus dem Geologisch – Paleontologischen Institut der Universitat Hamburg, 1985, p. 569.
41. Collins, C., Turpin, J., Betaux, A., Desparaires, C. and Kissel, C., Erosional history of the Himalayan and Burman range during the last two glacial–interglacial cycles. *Earth Planet. Sci. Lett.*, 1999, **171**, 647–660.
42. Chauhan, O. S., Rajawat, A. S., Pradhan, Y., Suneethi, J. and Nayak, S. R., Weekly observations on dispersal and sink pathways of the terrigenous flux of the Ganga–Brahmaputra in the Bay of Bengal during NE monsoon. *Deep-Sea Res. II*, 2004, in press.

ACKNOWLEDGEMENTS. We thank the Directors of NIO and IIG for providing facilities. We thank M. Samthien and E. Vogelsang, University of Kiel for carbon and oxygen isotopic analysis and interpretation. This is NIO contribution no. 3890.

Seismic reflection data: their utility in estimation of gas hydrates in deep marine sediments

Uma Shankar, N. Satyavani, Babita Sinha and N. K. Thakur*

National Geophysical Research Institute, Uppal Road, Hyderabad 500 007, India

The occurrence and significance of low-velocity sedimentary layer corresponding to free gas in the sediment beneath the bottom simulating reflector have long been a subject of debate. Either velocity or amplitude information in isolation is inadequate to estimate hydrate concentration. Reduction in amplitude (amplitude blanking) calibrated by interval velocity has been used to quantify hydrate concentration in the Kerala–Konkan area of western continental margin of India. The tentative estimate of hydrate in the representative sediment has been made using the time-average equation, in which the velocity structure of pure methane hydrate is inferred from the seismic data and known properties of pure hydrate.

A bottom simulating reflection (BSR) at a depth corresponding approximately to the base of the methane hydrate stability field is the most widely used indicator for the probable presence of gas hydrate accumulations beneath the sea bed. BSRs are observed worldwide on reflection seismic data from continental margins^{1,2}. Models have been developed to estimate the amount of hydrate or free gas associated with BSR^{3–6}. Only few of these models are constrained by independent drilling or laboratory data. An important indicator of the gas hydrates is the amplitude reduction or blanking observed above the BSR in seismic reflection profiles from the region of known hydrates. The marked decrease in amplitude above the BSR was related to a reduction in impedance contrast across sedimentary interfaces caused by the presence of hydrates^{7,8}.

Seismic reflection data suggest that an extensive accumulation of gas hydrate underlies the western continental margin of India (WCMI) in the Kerala–Konkan basin⁹. These gas hydrate accumulations are inferred from the presence of a BSR that lies 400 ms two-way travel time (TWT) beneath the seafloor (Figure 1). This depth closely approximates the base of the methane hydrate stability field⁹, indicating that this strong reflection event marks the base of hydrate-bearing sediments. The high reflection amplitude and reverse reflection polarity of the BSR with respect to the sea floor reflection allow us to infer the base of the hydrate.

Two types of analysis have been undertaken in this study: (i) Analysis of the BSR reflection amplitude and the nature of the BSR, and the inference of hydrate layer

*For correspondence. (e-mail: nkthakur@ngri.res.in)

from the amplitude variation with offset (AVO) analysis, and (ii) Saturation estimation through time-average equation. The nature of the BSR is studied through seismic modelling of its amplitude and waveform with varying source–receiver offsets. AVO analysis appears to be an important indicator to infer free gas below the gas hydrate and has been an increasingly important technique in the oil and gas industry for the last decade. The AVO method has been used in recent hydrate BSR studies^{3,10–12}.

Seismic line K-743 from the Kerala–Konkan basin (Figure 2) which shows a strong BSR (Figure 1) was studied in detail. The amount of gas hydrates in marine sediment is estimated using the method of Laberg *et al.*¹³. Our approach uses the interval velocity of the wave field. The increase in interval velocity is attributed to hydrate, and a decrease in interval velocity to regions where hydrate is absent.

The seismic reflection data (Figure 1) used in this study were collected over the WCMI in the early 1990s for the exploration of hydrocarbons by ONGCL. The data were made available to us by the Gas Authority of India (GAIL), to reprocess with suitable parameters and identify possible locations of gas hydrate-bearing horizons in this area. The acquisition system included a 96-channel seismic streamer with a maximum offset of 2575 m (active section) and air gun array source (total volume of 1650 cubic inches). The 48-fold data were reprocessed in the present study to preserve relative reflection amplitude. Data processing was carried out using ProMAX-2D seismic software on SUN workstations. A band-pass filter in the range 8–10 to 60–70 Hz was applied to the data. True amplitude recovery was done at 6 dB/s. Velocity analysis was conducted every 2 km in general, and at specific promising locations it was performed at an interval of 1 km. A spiking deconvolution was carried out to increase resolution.

The WCMI is a typical passive continental margin, which was generated during the break-up of eastern

Gondwana and the separation of Madagascar, and later the Seychelles from India about 80–65 Ma¹⁴. The continental shelf of the WCMI is more than 300 km wide in the northern region off Mumbai and narrows down to 50–60 km off Kerala coast in the south. The southern section of the WCMI is the Chagos–Laccadive volcanic ridge (CLR), which was emplaced as a consequence of the movement of the Indian Ocean lithosphere over the Reunion hot spot trace¹⁵. Most of the BSRs identified along the WCMI are located either along the continental slopes or along the flanks of the CLR¹⁶. Of particular interest are the acoustic wipeouts noticed at four locations in the western offshore region, which underlie the BSRs^{17,18}.

A strong reflection at 2950 ms TWT is observed on one of the lines K-743 (Figure 1). The general seismic characteristics for the observed BSRs associated with the base of the gas hydrate stability zone are listed as follows:

- (i) The BSR has strong reflection amplitude and reversed polarity relative to the sea floor reflection (Figures 1 and 3). Therefore, the BSR marks an interface at which there is a significant decrease in acoustic impedance.
- (ii) Blanking evidence is seen on the plot of normalized amplitude (in dB) versus absolute offset (Figure 4).

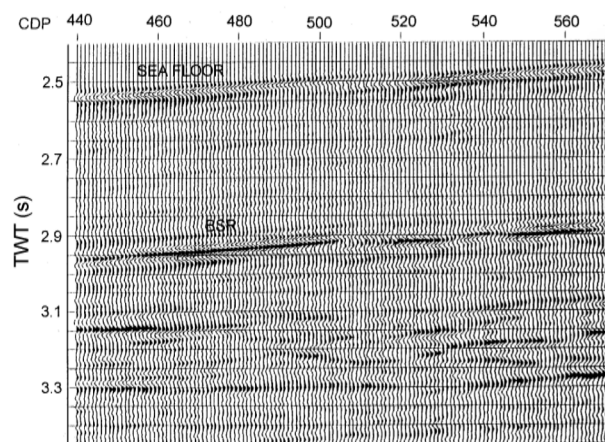


Figure 1. Seismic stack section along the line of study.

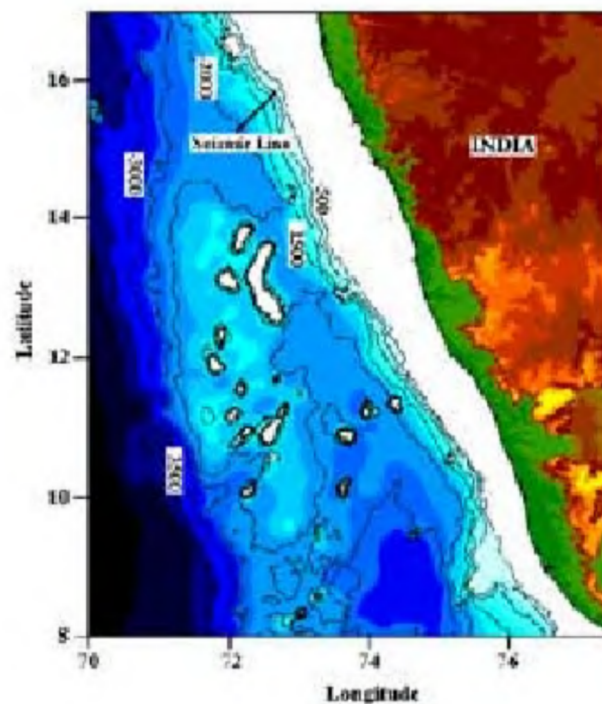


Figure 2. Study area in the Kerala–Konkan offshore, Western Continental Margin of India. Solid line indicates the location of the seismic line under study. Contours represent bathymetry over the region from GECO data.

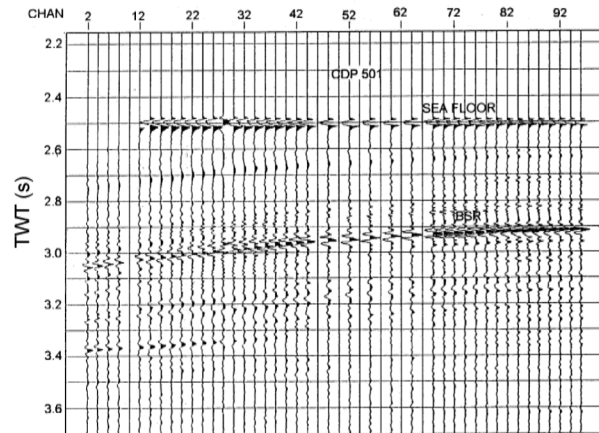


Figure 3. Common depth point gather of CDP 501, with normal move-out from study area.

- (iii) The bedding planes in this area are parallel to the sea floor; hence the cross-cutting phenomenon generally associated with BSR is not evident.
- (iv) Amplitude just below the BSR reflection is quite strong, indicating a sharp contrast in the velocity that point towards the base of a free gas layer.

True-amplitude processing technique with wavelet deconvolution were applied to optimize the quantitative analysis of the hydrated sediment. The processing was performed by the automatic editing method based on the median amplitude in a common depth point (CDP) gather¹⁹, with only a spherical spreading correction. Other amplitude corrections that compensate for effects such as attenuation and transmission loss were not included in this true-amplitude processing, because they may introduce seismic artifacts that impede identification of the hydrated sediment.

Our amplitude analysis was done in the two zones: either the interval between the sea floor and BSR, or the 400-ms thick section immediately overlying the BSR. Amplitude changes are based on calculation of the median reflectance defined as the envelope amplitude calibrated by the reflection amplitude. Details of amplitude variation near the BSR can be examined using plots similar to those shown in Figure 4. Here each dot represents the amplitude in an 8-ms window for five consecutive CDPs. The solid line is the five-point median of the average amplitude of five consecutive CDPs. In other words, the solid line is the running average of reflection amplitude over a moving window that is 32 ms in duration vertically by five CDPs horizontally. The decibel scale was computed on the basis of the most convenient reflection amplitude for the plot; therefore, we can get an absolute value of the reflection amplitude (i.e. reflectance) directly from the plot. Although the magnitude of the reflectance varies with the degree of interference and frequency con-

tent on band-pass-filtered seismic sections such as those used in this study, it is a useful quantity in comparing relative reflection strength along the line.

Variation of the *P*-wave reflection AVO amplitude versus offset or reflection amplitude versus angle is an important indicator of the presence of free gas at an interface. AVO studies carried out by earlier workers^{20,21} proved useful in determining the concentration and vertical distribution of gas hydrates. The reflection amplitude as a function of source–receiver offset depends on the compressional velocity (V_p), the shear velocity (V_s) and the Poisson's ratio (PR). The AVO depends primarily on PR, i.e. V_p/V_s . The compressional waves travel from the sediment with or without hydrate have normal PR and the sediment containing free gas with a low PR. This change in PR gives rise to amplitude that becomes substantially larger with increasing offset/incident angle. Thus, AVO can be an important indicator of free gas at an interface.

Successful evaluation of the AVO results requires removing the effects of geometric spreading, variation in shot and receiver coupling, ground roll, transmission losses, etc. on the amplitude. A number of corrections²² are necessary to compensate for all these effects and to obtain the true AVO data. Air-gun source and hydrophone receiver array attenuation are the most important for BSR analysis. The hydrophone array attenuation depends on the incident angle, since the near hydrophone in each group receives the signal slightly earlier than the far hydrophones. For a maximum angle of incidence of 45° on the air-gun array, the amplitude reduction³ is about 20%. For the seismic streamer, attenuation is primarily dependent on the array length.

Figure 3 illustrates the AVO behaviour. A significant increase in amplitude with the offset can be seen distinctly. AVO plots for a group of five CDP gathers from 501 to 504 are shown in Figure 5a and b. Figure 5a shows AVO response of the sea floor, while Figure 5b shows the response of the BSR. The figure incorporates the AVO response both before and after the directivity corrections. The increase in amplitude is demonstrated clearly in the plots that have been corrected for directivity. It may also be observed that the increase in BSR reflection amplitudes is quite significant when compared to sea floor reflection amplitudes after the directivity corrections.

The effect of gas hydrates can be explained using the time-average equation. Timur²³ first proposed three-phase time-average equation to explain the compressional wave velocity in various consolidated rocks measured at permafrost (sub-zero) temperatures. Pearson *et al.*²⁴ later applied the equation to hydrated rocks and concluded that it qualitatively explains the known sonic properties of hydrated sediment in consolidated media. They used the following three-phase time-average equation for velocity:

$$\frac{1}{V_p} = \frac{\phi(1-S)}{V_w} + \frac{\phi S}{V_h} + \frac{(1-\phi)}{V_m},$$

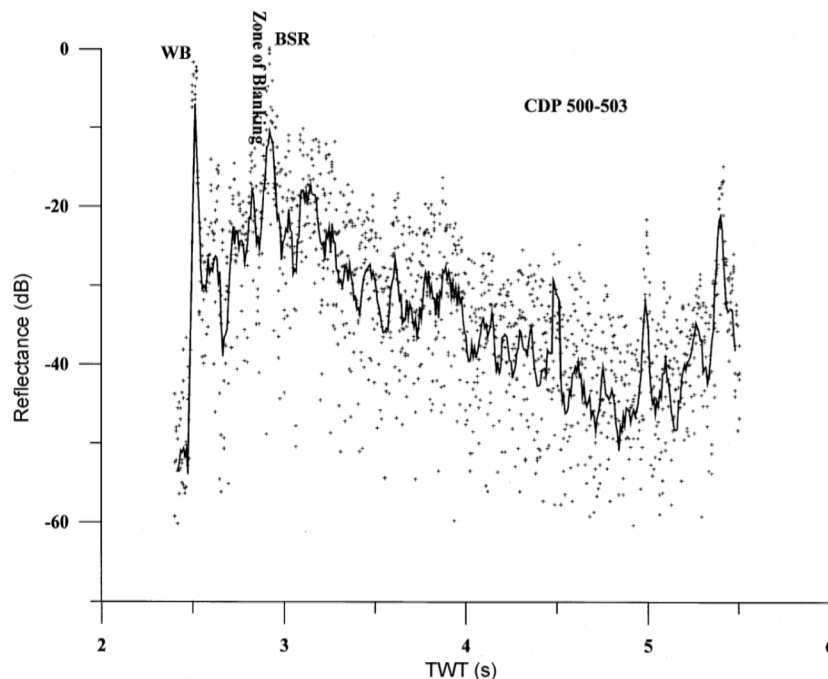


Figure 4. Graph showing amplitude analysis for selected CDP interval for line K-743 (shown in Figure 1). Each dot represents the amplitude of an 8-ms window and the solid line represents a four-point running median of four consecutive CDPs 501–503.

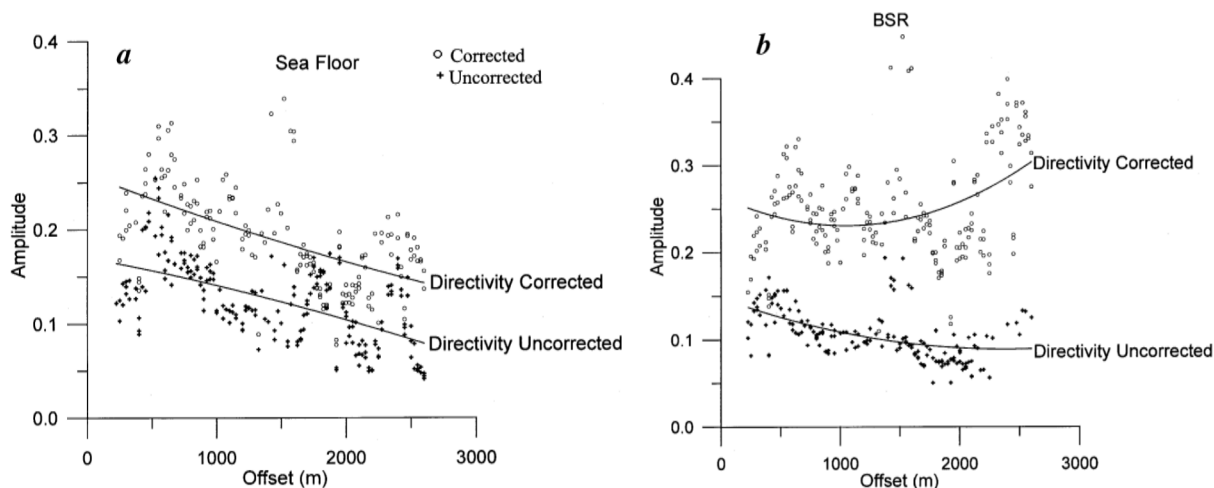


Figure 5. *a*, AVO plot of the sea floor for a group of five CDPs and their average corrected for directivity. *b*, AVO plot of the BSR for a group of five CDPs and their average, corrected for directivity. Open circles indicate amplitude values corrected for directivity and (+) indicates values uncorrected for directivity.

where V_p is compressional velocity of the hydrated sediment, V_h is compressional velocity of the pure hydrate, V_w is compressional velocity of the fluid, V_m is compressional velocity of the matrix, ϕ is porosity (as per cent) and S is the concentration of hydrate in the pore space (as per cent).

We used the above time-average equation to estimate the porosities from the interval velocities. Figure 6*a* and *b* shows the estimated interval velocity profiles through the zone of BSR and through the region immediately outside the BSR respectively, for two gathers each. The average interval velocity at the depth of the BSR is found to

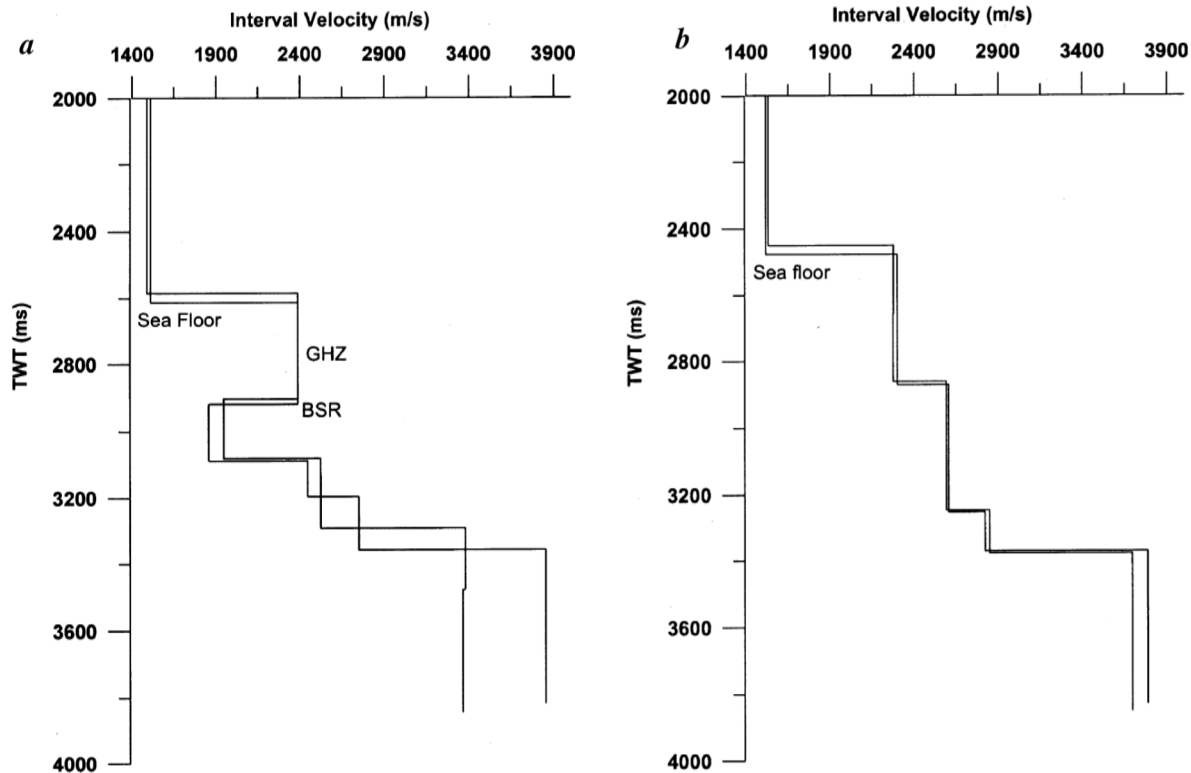


Figure 6. *a*, Estimated interval velocity profiles through BSR segments based on two constant velocities gather plots. Interval velocity profiles are calculated using Dix formula. GHZ, Inferred gas hydrate zone. *b*, Estimated interval velocity immediately outside the BSR reflections.

be around 2250 ms^{-1} from Figure 6*a*. It has been reported that in the absence of gas hydrate, the *P*-wave velocities derived from the effective medium theory and from the weighted equation are agreeable²⁵ if the porosity is around 30%. We assume that the average porosity within the sediments is around 30%. Velocity of the unsaturated rock away from the gas hydrate zone has been calculated to be 2864 m/s from the equation $1/2250 = 0.7/x + 0.3/1500$, where the water velocity (V_w) is 1500 m/s.

The compressional (*P*-wave) velocity of the pure hydrate has been estimated²⁶ to be 3300–3800 m/s. Assuming that the observed velocity increase from 2250 to 2450 m/s immediately above the BSR is due to the presence of gas hydrates, a first approximation of the volume comprising gas hydrate can be obtained from the time-average equation: $1/2450 = (0.7/2864) + (0.3 - y/1500) + (y/3300)$, where gas hydrate velocity (V_h) is considered to be 3300 m/s. From this calculation, 12% of the bulk (total) sediment volume or 40% of the pore volume comprises of gas hydrate. Using the gas hydrate velocity of 3800 ms^{-1} implies that the gas hydrate comprises 10% of the bulk volume or 34% pore volume.

According to the calculated relationship for the bulk density and compressional wave velocity, Gasman²⁷ and

Zimmerman and King²⁸ predict that the interval velocity of 2450 m/s indicates a hydrate saturation of about 24% of pore space or about 7% of the bulk volume.

We have proposed quantitative estimate of the bulk volume of gas hydrates in the zone above the BSR. Figure 4 relates amplitude blanking of seismic velocity, concentration of gas hydrate in pore spaces, and the concentration of representative hydrated sediments above and below a reflecting surface. Our results are consistent with the amplitude blanking and average interval velocities measured in the Kerala–Konkan area of WCMI from multi-channel seismic data. Estimation of the volume of hydrates (or methane) contained within the sediment above the BSR can be made from the hydrate concentrations.

The primary effect of hydrate concentration on the acoustic properties of marine sediment is an increase in interval velocity. Quantitative analysis of interval velocity can be used to estimate the bulk volume of gas hydrates. Another seismic attribute of hydrate concentration is amplitude blanking (Figure 4). This phenomenon is observed on WCMI; a reflection seismic section clearly shows the presence of the BSR. Attempts have been made to estimate the hydrate saturation using this seismic section. AVO studies have been made in order to ascertain

the mode of formation of the BSR. The presence of a low velocity layer may be indicative of the presence of brine-saturated sediment or a thin layer saturated by free gas. Initial estimates show that the gas hydrate saturation may be in the range 10–12% of the bulk volume. The estimates derived from theoretical studies are lower, around 7% of the bulk volume.

- Kvenvolden, K. A. and Barnard, L. A., Hydrates of natural gas in continental margins. In *Studies of Continental Margin Geology* (eds Watkins, J. S. and Drake, C. L.), Am. Assoc. Pet. Geol. Mem., 1983, vol. 34, pp. 631–640.
- Kvenvolden, K. A., Gas hydrates – geological perspective and global change. *Rev. Geophys.*, 1993, **31**, 173–187.
- Hyndmann, R. D. and Spence, G. D., A seismic study of methane hydrate marine bottom simulating reflectors. *J. Geophys. Res.*, 1992, **97**, 6683–6698.
- Miller, J. J., Lee, M. W. and Huene, R., An analysis of a seismic reflection from the base of a gas hydrate zone, offshore Peru. *Am. Assoc. Pet. Geol. Bull.*, 1991, **75**, 910–924.
- Singh, S. C., Minshull, T. A. and Spence, G. D., Velocity structure of a gas hydrate reflector. *Science*, 1993, **260**, 204–207.
- Minshull, T. A., Singh, S. C. and Westbrook, G. K., Seismic structure at a gas hydrate reflector, offshore western Colombia, from full waveform inversion. *J. Geophys. Res.*, 1994, **99**, 4715–4734.
- Shipley, T. H. *et al.*, Seismic evidence for widespread possible gas hydrate horizons on continental slopes and rises. *Am. Assoc. Pet. Geol. Bull.*, 1979, **63**, 2204–2213.
- Dillon, W. P., Booth, J. S., Paull, C. K., Fehlhaber, K., Hutchinson, D. R. and Swift, B. A., Mapping sub-seafloor reservoirs of a greenhouse gas – methane hydrates: In Proceedings of International Symposium on Marine Positioning (eds Kumar, M. and Maul, G. A.), Marine Geodesy Committee, Marine Technology Society, Washington DC, 1991, pp. 545–554.
- Reddi, S. I., Thakur, N. K., Ashalatha, B. and Sain, K., Reprocessing of multi-channel seismic data of ONGCL for gas hydrate exploration in offshore Goa. NGRI Technical Report No. 2001-EXP-30, 2001.
- Bangs, N. L. B., Sawyer, D. S. and Golovchenko, X., Free gas at the base of the gas hydrate zone in the vicinity of the Chile Triple Junction. *Geology*, 1993, **21**, 905–908.
- Ecker, C. and Lumley, D. E., AVO analysis of methane hydrates seismic data. *Full Meet. Suppl., Eos Trans. AGU*, 1993, **74**, 370.
- Andreassen, K., Hart, P. E. and Grantz, A., Seismic studies of a bottom simulating reflection related to gas hydrate beneath the continental margin of the Beaufort Sea. *J. Geophys. Res.*, 1995, **100**, 12659–12673.
- Laberg, J. S., Andreassen, K. and Knutesn, S. M., Inferred gas hydrate on the Barents Sea shelf – a model for its formation and a volume estimate. *Geo-Mar. Lett.*, 1998, **18**, 26–33.
- Norton, I. O. and Sclater, J. G., A model for the evolution of the Indian Ocean Breakup of Gondwanaland. *J. Geophys. Res.*, 1979, **84**, 6803–6830.
- Ashalatha, B., Subramanyam, C. and Singh, R. N., Origin and compensation of Chagos–Laccadive Ridge, and bathymetry data. *Earth Planet. Sci. Lett.*, 1991, **105**, 47–54.
- Veerayya, M., Karisiddaiah, S. M., Vora, K. H., Wagle, B. G. and Almeida, F., Gas hydrate: relevance to world margin stability and climate change. *J. Geol. Soc. India*, 1998, **137**, 239–253.
- Gupta, H. K. *et al.*, Analysis of single channel seismic data along the continental margin of India for gas hydrates. NGRI Technical Report No. 98-Lithos-221, 1998.
- Rao, Y. H., Subramanyam, C., Rastogi, A. and Deka, B., Anomalous features related to gas/gas hydrate occurrences along the western continental margins of India. *Geo-Mar. Lett.*, 2001, **21**, 1–8.
- Lee, M. W. and Hutchinson, D. R., True-amplitude processing techniques for marine, crustal-reflection seismic data. *U.S. Geol. Surv. Bull.*, 1990, **22**.
- Ecker, C., Dvorkin, J. and Nur, A. M., Sediments with gas hydrates: Internal structure from seismic AVO. *Geophysics*, 1998, **63**, 1659–1669.
- Andreassen, K., Hart, P. E. and MacKay, M., Amplitude versus offset modeling of the bottom simulating reflection associated with submarine gas hydrates. *Mar. Geol.*, 1997, **137**, 25–40.
- Ostrander, W. J., Plane wave reflection coefficients for gas sands at non-normal angles of incidence. *Geophysics*, 1984, **49**, 1637–1648.
- Timur, A., Velocity of compressional waves in porous media at permafrost temperature. *Geophysics*, 1968, **33**, 584–595.
- Pearson, C. F., Halleck, P. M., McGulre, P. L., Hermes, R. and Mathews, M., Natural gas hydrates, a review of *in situ* properties. *J. Phys. Chem.*, 1983, **87**, 4180–4185.
- Lee, M. W. and Collett, T. S., Comparison of elastic velocity model for gas hydrate bearing sediments. In *Natural Gas Hydrate: Occurrence, Distribution and Detection* (eds Paull, C. K. and Dillon, W. P.), AGU Monograph Series, 2001, vol. 124, pp. 179–189.
- Sloan, E. D., *Clathrate Hydrates of Natural Gases*, Marcel Dekker Inc., New York, p. 641.
- Gasmann, F., Über die elastizität poroser median. *Vierteljahrsschr Naturforsch. Ges. Zuerich*, 1951, **96**, 1–13.
- Zimmerman, R. W. and King, M. S., The effect of the extent of freezing on seismic velocities in unconsolidated permafrost. *Geophysics*, 1986, **51**, 1285–1290.

ACKNOWLEDGEMENTS. We thank Dr V. P. Dimri, Director, NGRI for permission to publish this paper. We also thank GAIL for making available the seismic data of this region.

Received 12 January 2004; revised accepted 10 May 2004

Coda duration magnitude scale of 2001 Bhuj aftershocks, India

P. Mandal*, R. Narsaiah, P. S. Raju and R. K. Chadha

National Geophysical Research Institute, Uppal Road, Hyderabad 500 007, India

Analogue seismograms of 120 aftershocks of magnitude exceeding 4.0 recorded on the short-period vertical seismometer at Hyderabad seismic observatory have been used to obtain a coda duration magnitude scale for Bhuj earthquakes, which includes the higher order terms of $\log_{10}\tau$, where τ is the coda length in seconds. In order to reduce the ambiguity in estimating coda duration, four background noise levels (1, 2, 6 and 10 mm) are experimented. We found that the duration magnitudes for 2 mm background level are more stable than those for 1, 6 and 10 mm. The new coda duration magnitude (M_d) scale for 2 mm level was obtained using regression analysis. The estimated M_d values are

*For correspondence. (e-mail: prantik_2k@hotmail.com)